nature cell biology

Actin dynamics counteract membrane tension during clathrin-mediated endocytosis

Steeve Boulant[1,2,4], Comert Kural[1,2,4], Jean-Christophe Zeeh[1,2], Florent Ubelmann[3] and Tomas Kirchhausen[1,2,5]

Clathrin-mediated endocytosis is independent of actin dynamics in many circumstances but requires actin polymerization in others. We show that membrane tension determines the actin dependence of clathrin-coat assembly. As found previously, clathrin assembly supports formation of mature coated pits in the absence of actin polymerization on both dorsal and ventral surfaces of non-polarized mammalian cells, and also on basolateral surfaces of polarized cells. Actin engagement is necessary, however, to complete membrane deformation into a coated pit on apical surfaces of polarized cells and, more generally, on the surface of any cell in which the plasma membrane is under tension from osmotic swelling or mechanical stretching. We use these observations to alter actin dependence experimentally and show that resistance of the membrane to propagation of the clathrin lattice determines the distinction between 'actin dependent and 'actin independent'. We also find that light-chain-bound Hip1R mediates actin engagement. These data thus provide a unifying explanation for the role of actin dynamics in coated-pit budding.

The coordinated action of a large number of structural and regulatory proteins and lipids is required for the assembly–disassembly of a clathrin-coated vesicle. Budding coated pits and other clathrin-coated structures can be followed in living cells by labelling component proteins with fluorescent markers[1–7]. Recent live-cell imaging studies reveal unexpected modes of endocytic coat assembly, with distinct kinetics, recruitment of associated proteins, requirements for the participation of actin and its accessory proteins, and mechanisms of membrane deformation[7–13].

Electron microscopy of B-lymphoblastoid cells showed association of actin microfilaments with clathrin-coated structures[14], indicating that actin may participate in coated-vesicle assembly by pulling the membrane inward. In cultured mammalian cells, actin polymerization is usually dispensable for coated-pit formation[7,15], but in some circumstances actin and a subset of regulators of short-branch actin assembly, including Arp2/3 (actin-related protein-2/3), cortactin and N-Wasp (also known as Wasl, Wiskott-Aldrich syndrome-like; refs 16–19), are recruited to clathrin-containing structures at or near the time of membrane scission. One such actin-dependent structure, termed a coated plaque, assembles at adherent surfaces of cultured mammalian cells[11,20]. Actin dynamics are essential for membrane invagination and scission associated with coated-plaque uptake. Actin dynamics also rescue the clathrin-mediated uptake of elongated (180 nm) vesicular stomatitis virus particles[6] (VSV), which block closure of the curved pit, causing endocytosis to stall. Coordinated actin polymerization and inward movement of the partially clathrin-coated virus narrows the neck between the pit and the plasma membrane, leading to dynamin-induced scission. Thus, actin assembly is a pathway required under stringent conditions, rather than an essential process under more permissive ones[10]. In contrast, clathrin-mediated internalization is constitutively actin dependent in yeast cells[9] where actin dynamics are needed to counteract the inhibition of endocytosis induced by elevated membrane tension[21].

Inhibition of actin dynamics blocks endocytosis from the apical but not the basolateral surface of polarized cells[22–29]. We sought an explanation for this difference by combining live-cell, spinning-disc confocal imaging with electron microscopy. We show in polarized MDCK cells, that pharmacologically inhibiting actin dynamics or disrupting the link between actin and clathrin (by blocking the interaction between clathrin and Hip1R, Huntingtin interacting protein 1 related; refs 11,30) selectively traps apical clathrin-coated pits at a late stage of assembly. More generally, if we raise membrane tension and inhibit actin dynamics, coated pits stall at a late stage of assembly in BSC1 or MDCK cells. Local actin dynamics seem to prevent stalling by imparting additional constriction force.

We compared the dynamics of endocytic clathrin adaptor protein 2 (AP-2)-coated structures at the apical and basolateral surfaces of polarized MDCK cells[1] (Fig. 1a). Most fluorescent AP-2 spots on the

[1]Department of Cell Biology, Harvard Medical School, Boston, Massachusetts 02115, USA. [2]Immune Disease Institute and Program in Cellular and Molecular Medicine at Children's Hospital, Boston, Massachusetts 02115, USA. [3]Laboratoire de Morphogénèse et Signalisation Cellulaires, Institut Curie Paris, Paris, Cedex 05, France. [4]These authors contributed equally to this work.
[5]Correspondence should be addressed to T.K. (e-mail: kirchhausen@crystal.harvard.edu)

Received 21 January 2011; accepted 27 June 2011; published online 14 August 2011; DOI: 10.1038/ncb2307

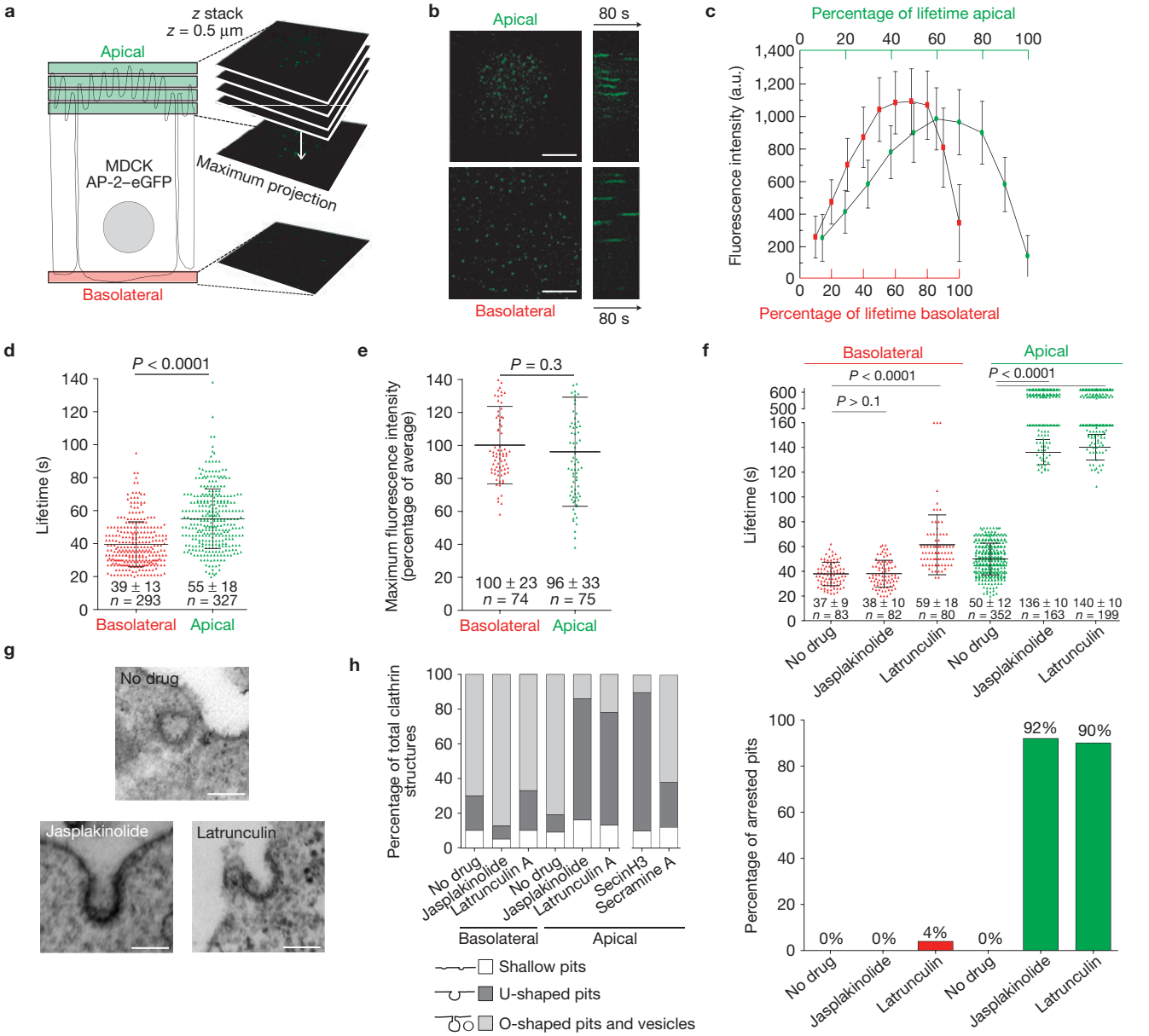

Figure 1 Formation of endocytic coated pits and vesicles at the apical and basolateral surfaces of polarized MDCK cells. (**a**) Imaging procedures used to visualize the dynamics of pit formation at the apical and basolateral surfaces of polarized MDCK cells. Movies from the dome-like apical surface are from 3D time series acquired at 2 s intervals from 3–5 serial optical sections spaced by 0.5 µm and using 100 ms exposures; 2D time series were created from maximum-intensity *z*-projection sets. Movies from the basolateral surface are 2D time series acquired at 2 s intervals from a single optical section. (**b**) Snapshot from a maximum-intensity projection (left) and representative kymograph (right) of coated-pit formation at the apical and basolateral surfaces from the same polarized MDCK cell; AP-2 labelled with σ2–eGFP; scale bars, 5 µm. (**c**) Average fluorescence intensity of AP-2 structures forming at the apical and basolateral surfaces of polarized MDCK cells ($n = 3$), normalized to the lifetime of each individual pit analysed (percentage of lifetime). Each point represents average ± s.d. (**d**) Scatter plot of individual lifetimes of coated structures from seven polarized MDCK cells. Each data set represents average ±s.d. *n* is the number of objects analysed. Statistical significances for lifetime differences are shown. (**e**) Scatter plot of individual maximum fluorescence intensities for coated structures. (**f**) Scatter plots of lifetimes for individual AP-2 spots at the apical and basolateral surfaces of polarized MDCK cells stably expressing σ2–eGFP in the absence or presence of jasplakinolide or latrunculin A. The upper and lower data sets are from distinct time series of 10 and 2.5 min in duration, respectively. Bottom, fraction of AP-2 objects with longer duration than the time series (percentage of arrested pits). (**g**) Morphological analysis of clathrin-coated structures on the apical surface of polarized MDCK cells treated with jasplakinolide, latrunculin A, SecinH3 or secramine A. Representative electron microscopy images of the most abundant clathrin-coated-pit profiles. Scale bars, 100 nm. The coated structures were classified as shallow, U-shaped or nearly-mature Ω- and fully-mature O-shaped vesicles. (**h**) Relative frequency of profiles in about 45 cells per condition.

basolateral surface belonged to a single class of diffraction-limited objects, with the properties characteristic of canonical coated pits and vesicles, ~100–200 nm in diameter[1,5,7,11] (Fig. 1b,c and Supplementary Movie S1). Their mean lifetime was 39 ± 13 s (Fig. 1d). The mean lifetime of clathrin-coated pits on the apical surface of the same polarized MDCK cells was significantly longer (55 ± 18 s; $P < 0.001$;

Fig. 1d and Supplementary Movie S1), although both had a similar maximum fluorescence intensity (Fig. 1c,e) and hence reached a similar final size[1,11]. Disturbance of actin assembly in polarized MDCK cells with latrunculin or jaskplakinolide resulted in a marked increase in the lifetime of apical pits. About 90% of the pits arrested and remained for at least 10 min (the upper limit of the time series), and the remaining ~10% had lifetimes significantly longer than at the apical surface in non-treated cells (Fig. 1f and Supplementary Movie S2) and transferrin endocytosis ceased[22,23,25] (Supplementary Figs S1a,b). In contrast, basolateral pits from the same cells were unaffected by jaskplakinolide and showed a small increase in lifetime (from 37 s to 59 s) and in the fraction of arrested pits (from 0% to 4%) in response to latrunculin (Fig. 1f and Supplementary Movie S2). The dependence on actin dynamics required cell polarization. Incubation with jaskplakinolide did not affect the formation and lifetime of dorsal pits in non-polarized MDCK cells (Supplementary Fig. S2).

We ruled out the possibility that cessation of coat growth at the apical surface resulted from depletion of free cytosolic coat components by transiently exposing the cells to 1-butanol, which induces coat disassembly[7]. Incubation of jasplakinolide-treated polarized MDCK cells for 3 min with 1-butanol led to rapid disappearance (~10 s) of all AP-2 spots (Supplementary Fig. S3a, 1-butanol). Removal of the 1-butanol with jasplakinolide still present led to synchronous appearance of newly formed apical coated pits that again stalled at late assembly (Supplementary Fig. S3a,b). The fluorescence intensity of the long-lived apical pits in jaskplakinolide-treated cells was on average 10% less than the maximum intensity in untreated cells (Supplementary Fig. S3b). As fluorescence intensity is proportional to coat size[11], this indicates that the long-lived pits may arrest at a late stage of coat assembly, but before full completion. Electron microscopy of MDCK cells treated with jasplakinolide or latrunculin showed a substantial increase (from 10 to ~70%) in the fraction of coated pits at the apical surface linked to the plasma membrane by wide necks (U-shaped), representing incomplete coats arrested at a relatively late stage of assembly (Fig. 1g,h). Narrower necks were less common, and we saw no long tubules decorated at their end by clathrin coats. Untreated control cells showed the expected distribution of coated profiles (Fig. 1g,h). Jaskplakinolide or latrunculin did not affect the distribution of basolateral coated profiles (Fig. 1h). Dynamin associates with the neck of a fully formed coated pit and promotes release of a coated vesicle[1,4,31]. Dynamin does not associate with the wide neck of incomplete pits, and indeed very few (~5%) of the long-lived apical pits generated by jasplakinolide treatment recruited a detectable amount of dynamin-2 (Supplementary Fig. S4a,b). The apical pits of untreated cells recruited dynamin normally (~30% of pits co-localize with the relatively strong dynamin signal; Supplementary Fig. S4b). We conclude that clathrin-coated pits assembling on the apical surface of polarized MDCK cells require actin dynamics for closure but not for initiation, whereas coat assembly on the basolateral surface is actin independent.

We next examined the differential effects at the two surfaces of inhibiting the small GTPases Cdc42, Rac1 and Arf6 (regulators of Arp2/3-mediated actin polymerization[26,32]) and of blocking clathrin binding of Hip1R. Cdc42 inhibition did not arrest pit formation, had only a small effect on the formation and lifetime of apical or basolateral pits (Fig. 2a) and had no evident influence on the distribution of apical coat morphologies (Fig. 1h). Rac1 inhibition seemed to arrest apical-pit assembly, as a large fraction of the pits (60%) were present throughout the complete movie; it also retarded basolateral pit assembly by about twofold, with a modest effect on completion and budding (15% arrest). Arf6 has been linked to clathrin-based endocytosis in HeLa cells[33] and at the apical surface of polarized MDCK cells[24]. Arf6 inhibition similarly arrested most of the apical pits (76%), but had no detectable effect on basolateral coat dynamics. In all cases, the fluorescence intensity of the arrested coated pits was equivalent to the maximum intensity of pits imaged in untreated cells, indicating that the coats arrested at a late stage of assembly. Consistent with this conclusion, we found by electron microscopy an accumulation of U-shaped coats at the apical surfaces of polarized MDCK cells following SecinH3 treatment (Fig. 1h). These inhibitors had no effect on pit assembly in non-polarized MDCK cells.

Hip1R interacts with F-actin, cortactin and clathrin light chains[34–36] and connects the actin cytoskeleton with clathrin coats[34]. It is essential for assembly of coated plaques[11] and for endocytosis of VSV (ref. 6), but not for completion of coated pits in non-polarized cells[11]. We detected a role for Hip1R in apical-pit assembly by blocking the association of Hip1R with clathrin—either by overexpression of a dominant-negative form of clathrin light chain B (CLCb-EED/QQN), which binds the clathrin heavy chain but does not recruit Hip1R (refs 10, 11,30), or by depletion with short interfering RNA (siRNA) of both forms of the clathrin light chain. CLCb-EED/QQN overexpression in non-polarized cells does not inhibit clathrin-mediated endocytosis[11,30]; it prevents formation of clathrin-coated plaques, but not of coated pits[11]. Overexpression in polarized MDCK cells inhibited completion of apical pits (60% arrest, as defined by pits with lifetimes longer than the upper limit of the time series we recorded) but affected basolateral pits in the same cells only modestly, increasing their lifetimes from 47 s to 86 s and generally permitting complete assembly (15% arrest; Fig. 2b). Overexpression of wild-type LCb had no detectable effect on pit dynamics[11] (Fig. 2b), confirming that failure of the mutated light chain to recruit Hip1R had produced the observed late-stage arrest. siRNA-mediated knockdown of light chains led to late-stage arrest of pits at the apical but not at the basolateral surface (Fig. 2b). Results from Hip1R depletion were not interpretable because of the massive upregulation of the number of actin filaments throughout the cells[17,35,37] (Supplementary Fig. S3c), the increase in the level of cytosolic AP-2 and the general arrest of coated-pit formation at the apical and basolateral surfaces of polarized MDCK cells (Supplementary Fig. S3d), explaining the previously observed partial inhibition of transferrin uptake[35]. Thus, under actin-independent conditions, inhibiting Hip1R recruitment has no influence on clathrin-mediated endocytosis[30] or on coat assembly[11]. When actin dynamics are required to finish coat assembly, however, blocking Hip1R recruitment has the same effect (late-stage arrest) as blocking actin dynamics. As for Hip1R, the light chains are dispensable for initiation and early growth of coats under all conditions examined.

Apical surfaces of polarized epithelial cells have large numbers of microvilli. Treatment of polarized MDCK cells with a short hairpin RNA (shRNA) probe specific for ezrin, on which microvilli depend, resulted in substantial loss of the protein and disappearance of microvilli (Supplementary Fig. S5a). Following ezrin depletion, actin was no longer required for apical-pit completion (Supplementary Fig. S5b). Moreover, overexpression of villin-1–Cherry in non-polarized BSC1 cells generated a large number of microvilli-like

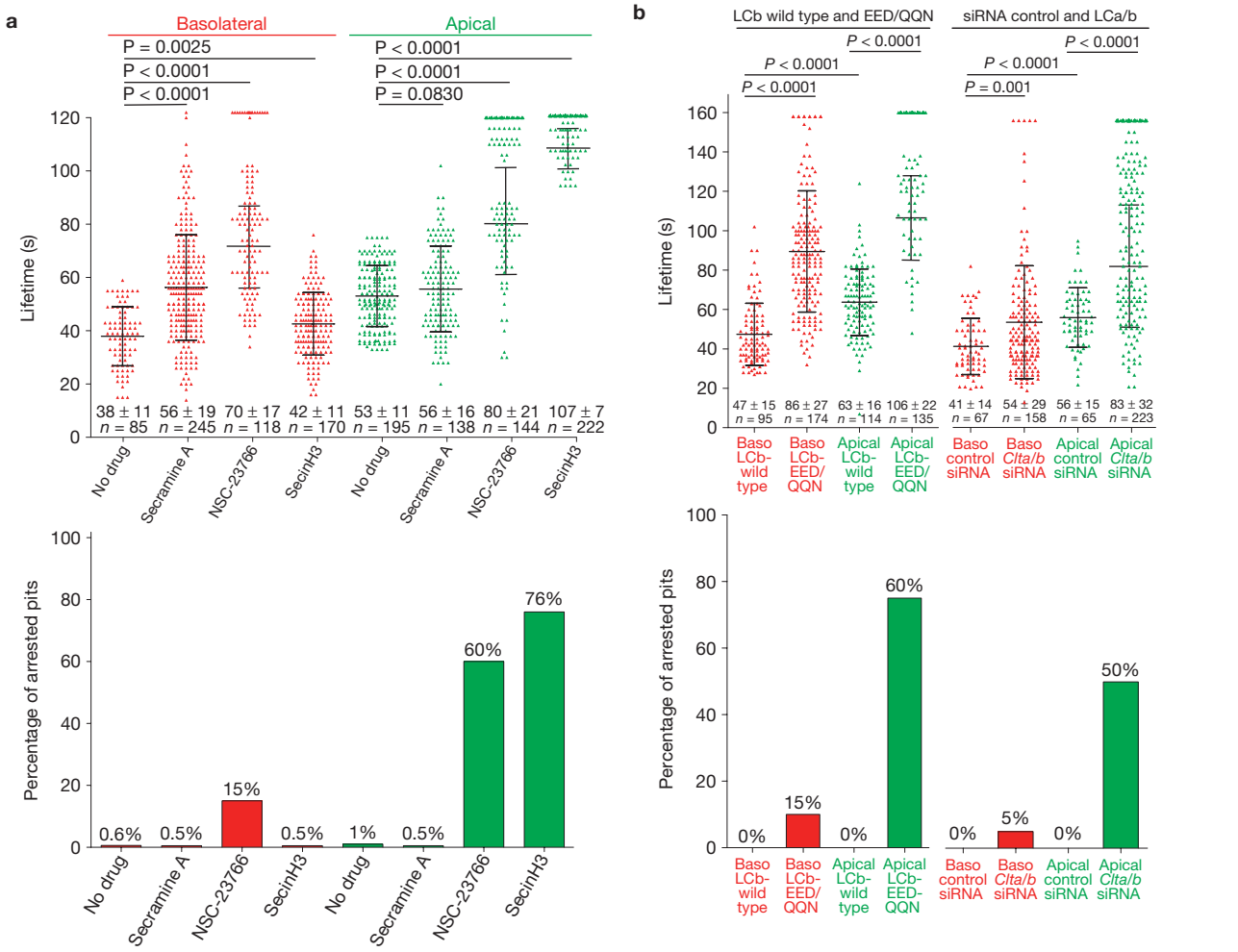

Figure 2 Disruption of apical coat formation by pharmacological interference with the small GTPases Rac1 and Arf6 and interference with the function of clathrin light chains. (**a**) Top, scatter plots of lifetimes for individual AP-2 spots. Polarized MDCK cells stably expressing σ2–eGFP were treated for 10 min before imaging with secramine A, NSC-23766 or SecinH3, small molecule inhibitors of Cdc42, Rac1 and Arf6, respectively. Each data set represents average ±s.d. for objects whose duration was fully included in the time series. *n* is the number of objects analysed. Statistical significances for the differences in lifetimes are shown. Bottom, fraction of AP-2 objects with longer duration than the time series. (**b**) Top, scatter plots of lifetimes for individual AP-2 spots imaged at the apical and basolateral (Baso) surfaces of polarized MDCK cells stably expressing σ2–eGFP and transiently expressing wild-type or mutant clathrin light chain B fused to Cherry (left) or depleted of both clathrin light chains by *Clta* and *Cltb* siRNA (right). Each data set represents average ±s.d. *n* is the number of objects analysed. Bottom, fraction of AP-2 objects with longer duration than the 160 s time series.

structures (Supplementary Fig. S5c) and caused actin-dependent coated-pit maturation (Supplementary Fig. S5d). Thus, the actin dependence of coat completion correlates with a property imparted to the plasma membrane in response to the formation of microvilli or microvillus-related structures.

Membrane tension in polarized cells is greater in apical than in basolateral regions[38]. We investigated whether clathrin-coat assembly might be sufficient to deform the underlying membrane completely under conditions of low membrane tension, whereas an additional activity associated with actin dynamics might be needed under conditions of high membrane tension. Increasing membrane tension by exposing cells to hypotonic medium (Fig. 3) revealed strong correlation between the severity of the hypotonic treatment and the appearance of arrested pits in non-polarized cells treated with jaskplakinolide (Fig. 3 and Supplementary Movie S3) and at the basolateral surface of polarized MDCK cells treated first with jasplakinolide (not shown). The actin requirement induced by hypotonic treatment was reversible (data not shown). Electron microscopy of jaskplakinolide-treated BSC1 cells incubated with hypotonic medium confirmed that most apical coated pits had U-shaped structures. The pits from these cells also failed to accumulate dynamin (not shown). We also increased membrane tension by laterally stretching cells growing on an elastic support. Pits at the basolateral surface of control, unstretched MDCK cells had an average lifetime of 43 s that was insensitive to jasplakinolide (Fig. 4b), comparable to pits in MDCK cells grown on glass coverslips (Fig. 1d). Linear stretching by 25% led to a small but statistically significant increase in pit lifetime (from 43 s to 52 s) and pit arrest (from 4% to 8%). Jaskplakinolide treatment of the stretched cells resulted in a marked increase in pit lifetimes and percentage of arrested pits (from 8% to 60%; Fig. 4b). Thus, local actin dynamics must coordinate with clathrin assembly to achieve complete vesiculation following increased membrane tension.

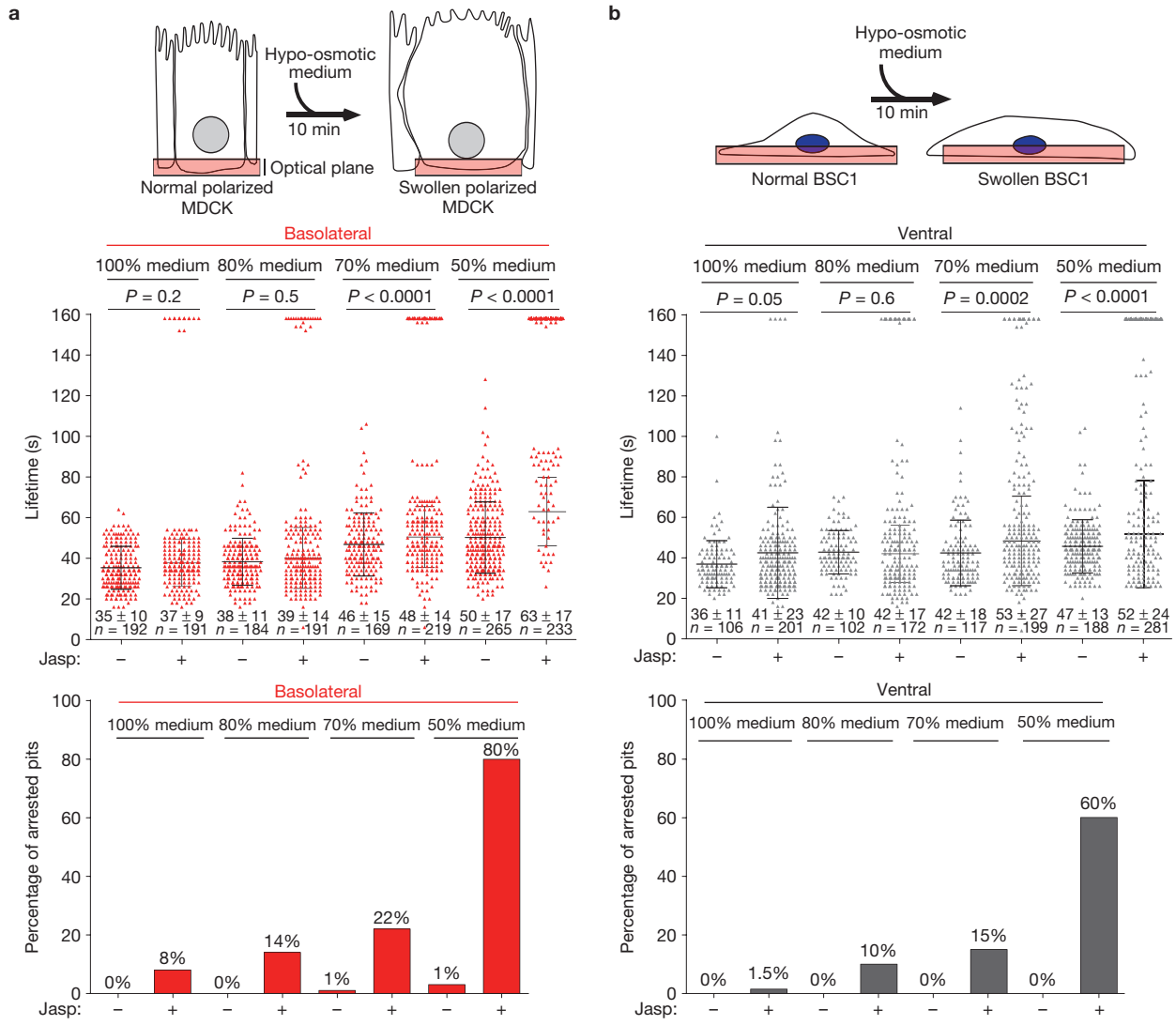

Figure 3 Actin dependence for endocytic coat formation in cells swelled by hypo-osmotic treatment. Polarized MDCK or non-polarized BSC1 cells incubated for 10 min in serially diluted medium (from 100% to 50%) of decreasing osmolarity, ranging from 311 to 174 mOsM, were analysed for the effects of altering actin dynamics on the lifetimes of their AP-2-coated structures. Each data set represents average ± s.d.; *n* is the number of objects analysed. (**a**) Top, schematic representation of polarized MDCK cells stably expressing σ2–eGFP exposed to hypo-osmotic medium. Middle, scatter plots of lifetimes for individual basolateral AP-2 spots of cells exposed for 10 min to hypo-osmotic media in the absence and presence of jasplakinolide (Jasp). Bottom, fraction of AP-2 objects with longer duration than the time series. (**b**) Top, schematic representation of BSC1 cells stably expressing σ2–eGFP exposed to hypo-osmotic medium. Middle, scatter plots of lifetimes for individual ventral AP-2 spots of cells exposed for 10 min to hypo-osmotic media in the absence and presence of jasplakinolide. Bottom, fraction of AP-2 objects with longer duration than the time series.

Thus, we show that interfering with actin dynamics induces arrest of canonical coated-pit assembly under some circumstances, but not under others. Indeed, actin activity is essential for efficient completion of coated pits at the apical surfaces of polarized cells in culture, but not at the basolateral surfaces of the same cells. Coat assembly in various non-polarized cells does not ordinarily depend on actin[7,11,15]. Furthermore, the actin dependence of coated-pit assembly can be modulated experimentally by modifying membrane tension: coat formation in a non-polarized cell can be rendered actin dependent by exposure to hypotonic medium, by stretching the substrate or by inducing the formation of microvillus-like structures; coat formation at the apical surface of a polarized cell can be rendered actin independent by shrinking its apical microvilli. In addition, interfering with actin dynamics under conditions that require actin activity causes coats to stall late in assembly. Most AP-2 complexes are recruited during earlier stages[11,20,39]. Therefore, we estimate (from the fluorescence intensity of tagged AP-2 and from the appearance of the U-shaped pits that accumulate) that the stalled coats are roughly two-thirds to three-quarters complete. At this stage of completion, the 'neck' is probably not yet narrow enough to allow dynamin recruitment, as the dynamin burst normally associated with maturation of a coated pit into a coated vesicle was not detected. Finally, we show that perturbing actin dynamics does not directly affect coat initiation[7]. Thus, canonical coated pits differ in this respect from coated plaques, which require actin dynamics for both initiation and invagination[11].

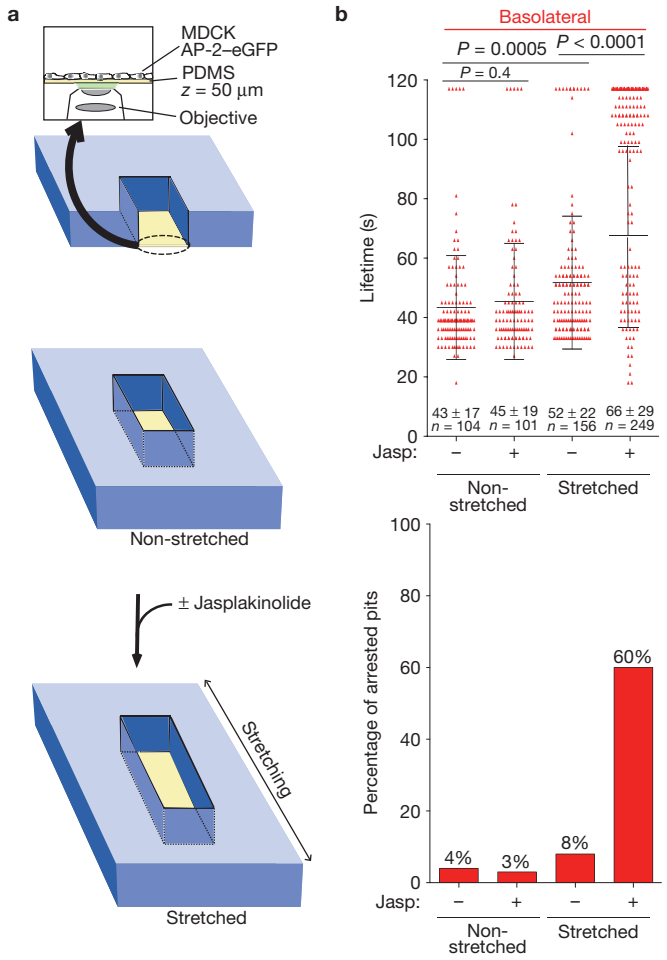

Figure 4 Actin dependence of endocytic coat formation in mechanically stretched cells. (**a**) Schematic representation of the device used to image mechanically stretched, non-polarized MDCK cells. An optically clear, stretchable silicon holder made of PDMS, about 50 μm thick, which could make contact with the oil above a ×63 objective lens was placed at the bottom of the stretching device. Cells were grown for 24 h on the PDMS surface pre-coated with fibronectin and then imaged by spinning-disc confocal microscopy; the spherical-aberration-correction device was essential for detecting the diffraction-limited coated structures containing AP-2–eGFP. (**b**) Dynamics of coated pits before and after ~25% linear stretching. Top, scatter plots for lifetimes of individual AP-2 spots from the ventral surface of cells subjected to controlled stretching in the presence or absence of jasplakinolide. Each data set represents average ± s.d. *n* is the number of objects analysed. Bottom, fraction of AP-2 objects with longer duration than the time series.

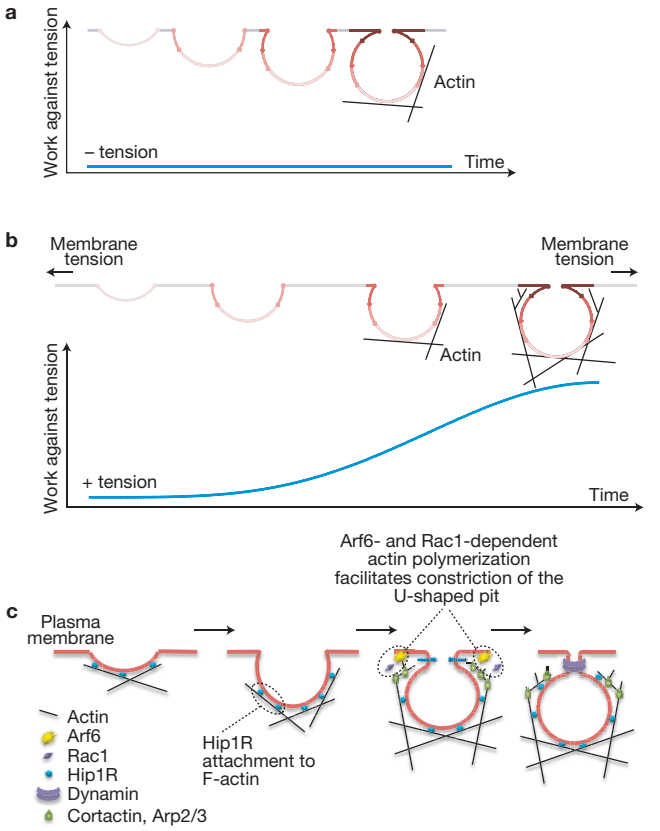

Figure 5 Model depicting the role of actin polymerization during the formation of endocytic clathrin-coated pits. (**a**) Under non-stringent conditions and low membrane tension, assembly of the clathrin coat is sufficient to deform the membrane into a tightly constricted coated pit. (**b**) Under more stringent conditions of high membrane tension, clathrin assembly is not sufficient and membrane invagination stalls; actin polymerization then provides the additional work needed to complete membrane bending. Hip1R links the assembling clathrin coat to actin polymers, and if sufficient time is allowed, then assembly of short-branched actin rescues the stalled coat. The two main forces resisting membrane deformation are bending and tension. The bending work per unit area depends inversely on the curvature and hence is uniform for a spherical or nearly spherical vesicle. The work done against a constant membrane tension depends on the net increase in membrane area—that is, the area of the invaginated membrane minus the area of the opening it covers. The plot represents the cumulative work required to counteract membrane tension, and does not include the work required to create the membrane vesicle. The cumulative work was calculated according to $W = \pi r^2 T(1-\cos\alpha)^2$, where T is the membrane tension and α is the angle (in radians) between the pole of the budding pit and the position at which the curved pit intersects the plane of the plasma membrane (see Methods). When the neck begins to constrict ($\alpha = \pi/2$), the area of the opening decreases and the net increase in area rises sharply. When the pit is complete, $\alpha = \pi$. (**c**) Hip1R links actin filaments with the clathrin coat by interactions with F-actin and clathrin light chains. Branched actin filaments grow towards the plasma membrane through new filament assembly at the barb end of the stabilized actin filaments; this growth relies on Arp2/3 stimulation, mediated by cortactin and by small GTPases such as Arf6 and Rac1.

We investigated what determines actin engagement if coat assembly stalls. In principle, there may be a 'sensor' of assembly arrest. Alternatively, actin may be engaged constitutively, but with at most a small contribution to observable coat dynamics except in circumstances of elevated membrane tension. The distinction between 'actin dependent' and 'actin independent' would then be determined by the threshold of membrane tension (or other resistance to propagation of the coat lattice) at which the free energy of clathrin–clathrin contacts can no longer overcome membrane resistance to generating a constricted neck. Our experiments, in which we switch from actin dependence to actin independence and vice versa, are consistent with this threshold picture. Indeed, increased tension is a common feature in which actin dynamics are required for coated-pit maturation beyond the 'U' stage. One explanation for why coated-pit assembly may stall at this point is embodied in Fig. 5. Under conditions of constant membrane tension, the work needed to invaginate the first hemisphere of a coated vesicle is substantially less than that needed to complete the second hemisphere (see Methods). Extreme levels of tension will

probably block invagination altogether; an intermediate level may stall the process when the work needed to counteract the tension is greater than incremental coat assembly can contribute.

Clathrin-mediated uptake in yeast cells depends constitutively on actin dynamics. Initial steps in coat formation precede local actin assembly, which is essential for invagination and inward movement[9]. Increased turgor diminishes internalization[21], in agreement with our observations on membrane tension in mammalian cells. Exposure to hyperosmotic medium, which reduces turgor to below-normal levels, rescues internalization of a fluid phase marker, even when actin dynamics are blocked[21], but it is not clear whether the rescue involves a clathrin-coated structure.

We have shown that actin polymerization takes over from clathrin polymerization in driving membrane invagination, when the latter process stalls. Actin is engaged at the coat by clathrin-light-chain-bound Hip1R. We have not determined whether actin simply pushes the plasma membrane away from the coat, or whether branching at Arp2/3 helps constrict the neck. Actin polymerization similarly takes over when clathrin polymerization and assembly stalls because of steric interference from cargo (for example, VSV; refs 6,10), and actin alone drives the remaining membrane invagination and constriction. Coated plaques are also examples of this phenomenon, in which adhesion of cell-surface proteins to the substrate generates the steric interference. □

METHODS

Methods and any associated references are available in the online version of the paper at http://www.nature.com/naturecellbiology

Note: Supplementary Information is available on the Nature Cell Biology website

ACKNOWLEDGEMENTS

This work was supported by NIH grant National Institutes of Health GM 075252 (T.K.) and a Harvard Digestive Disease Consortium Feasibility Award (S.B.). We express gratitude to E. Marino (supported by NIH grant U54 AI057159, New England Regional Center of Excellence in Biodefense and Emerging Infectious Diseases) for maintaining the imaging resource used in this study and to S.C. Harrison for help with describing the force contributed by membrane tension and for editorial assistance. We gratefully acknowledge M. Ericsson and I. Kim for preparation of samples for electron microscopic analysis and members of the Kirchhausen laboratory for thought-provoking discussions. We thank M. Arpin (Centre National de la Recherche Scientifique (CNRS)/Morphogenèse et Signalisation cellulaires, Paris, France) and C. Revenu (Centre National de la Recherche Scientifique/Institut Curie, Paris, France) for the antibody specific for villin-1. We also acknowledge S. Robine for important suggestions involving the villin-1/villin-2 depletion experiments.

AUTHOR CONTRIBUTIONS

S.B., C.K. and T.K. designed experiments; S.B. and C.K. carried out experiments; S.B. and C.K. analysed data; C.K. developed the analytical tools to analyse the 3D data. F.U. provided expression vectors specific for the experiments with villin-1/villin-2, contributed to the experimental design of the experiments involved in villin-1/villin-2 depletion and created the LLCPK1 cell line. S.B. and T.K. wrote the manuscript. All authors discussed the results and contributed to the final manuscript.

COMPETING FINANCIAL INTERESTS

The authors declare no competing financial interests.

Published online at http://www.nature.com/naturecellbiology
Reprints and permissions information is available online at http://www.nature.com/reprints

1. Ehrlich, M. *et al.* Endocytosis by random initiation and stabilization of clathrin-coated pits. *Cell* **118,** 591–605 (2004).
2. Conibear, E. Converging views of endocytosis in yeast and mammals. *Curr. Opin. Cell Biol.* **22,** 513–518 (2010).
3. Kaksonen, M., Toret, C. P. & Drubin, D. G. A modular design for the clathrin- and actin-mediated endocytosis machinery. *Cell* **123,** 305–320 (2005).
4. Merrifield, C. J., Feldman, M. E., Wan, L. & Almers, W. Imaging actin and dynamin recruitment during invagination of single clathrin-coated pits. *Nat. Cell Biol.* **4,** 691–698 (2002).
5. Boucrot, E., Saffarian, S., Zhang, R. & Kirchhausen, T. Roles of AP-2 in clathrin-mediated endocytosis. *PloS ONE* **5,** e10597 (2010).
6. Cureton, D. K., Massol, R. H., Saffarian, S., Kirchhausen, T. L. & Whelan, S. P. J. Vesicular stomatitis virus enters cells through vesicles incompletely coated with clathrin that depend upon actin for internalization. *PLoS Pathog.* **5,** e1000394 (2009).
7. Boucrot, E., Saffarian, S., Massol, R., Kirchhausen, T. & Ehrlich, M. Role of lipids and actin in the formation of clathrin-coated pits. *Exp. Cell Res.* **312,** 4036–4048 (2006).
8. Perrais, D. & Merrifield, C. J. Dynamics of endocytic vesicle creation. *Dev. Cell* **9,** 581–592 (2005).
9. Kaksonen, M., Toret, C. P. & Drubin, D. G. Harnessing actin dynamics for clathrin-mediated endocytosis. *Nat. Rev. Mol. Cell Biol.* **7,** 404–414 (2006).
10. Cureton, D. K., Massol, R. H., Whelan, S. P. J. & Kirchhausen, T. The length of vesicular stomatitis virus particles dictates a need for actin assembly during clathrin-dependent endocytosis. *PLoS Pathog.* **6,** e1001127.
11. Saffarian, S., Cocucci, E. & Kirchhausen, T. Distinct dynamics of endocytic clathrin-coated pits and coated plaques. *PLoS Biol.* **7,** e1000191 (2009).
12. Kirchhausen, T. Imaging endocytic clathrin structures in living cells. *Trends Cell Biol.* **19,** 596–605 (2009).
13. Mettlen, M. *et al.* Endocytic accessory proteins are functionally distinguished by their differential effects on the maturation of clathrin-coated pits. *Mol. Biol. Cell* **20,** 3251–3260 (2009).
14. Salisbury, J. L., Condeelis, J. S. & Satir, P. Role of coated vesicles, microfilaments, and calmodulin in receptor-mediated endocytosis by cultured B lymphoblastoid cells. *J. Cell Biol.* **87,** 132–141 (1980).
15. Fujimoto, L. M., Roth, R., Heuser, J. E. & Schmid, S. L. Actin assembly plays a variable, but not obligatory role in receptor-mediated endocytosis in mammalian cells. *Traffic* **1,** 161–171 (2000).
16. Merrifield, C. J., Perrais, D. & Zenisek, D. Coupling between clathrin-coated-pit invagination, cortactin recruitment, and membrane scission observed in live cells. *Cell* **121,** 593–606 (2005).
17. Le Clainche, C. *et al.* A Hip1R-cortactin complex negatively regulates actin assembly associated with endocytosis. *EMBO J.* **26,** 1199–1210 (2007).
18. Merrifield, C. J., Qualmann, B., Kessels, M. M. & Almers, W. Neural Wiskott Aldrich Syndrome Protein (N-WASP) and the Arp2/3 complex are recruited to sites of clathrin-mediated endocytosis in cultured fibroblasts. *Eur. J. Cell Biol.* **83,** 13–18 (2004).
19. Benesch, S. *et al.* N-WASP deficiency impairs EGF internalization and actin assembly at clathrin-coated pits. *J. Cell Sci.* **118,** 3103–3115 (2005).
20. Saffarian, S. & Kirchhausen, T. Differential evanescence nanometry: live-cell fluorescence measurements with 10-nm axial resolution on the plasma membrane. *Biophys. J.* **94,** 2333–2342 (2008).
21. Aghamohammadzadeh, S. & Ayscough, K. R. Differential requirements for actin during yeast and mammalian endocytosis. *Nature Cell Biol.* **11,** 1039–1042 (2009).
22. Gottlieb, T. A., Ivanov, I. E., Adesnik, M. & Sabatini, D. D. Actin microfilaments play a critical role in endocytosis at the apical but not the basolateral surface of polarized epithelial cells. *J. Cell Biol.* **120,** 695–710 (1993).
23. Jackman, M. R., Shurety, W., Ellis, J. A. & Luzio, J. P. Inhibition of apical but not basolateral endocytosis of ricin and folate in Caco-2 cells by cytochalasin D. *J. Cell Sci.* **107,** 2547–2556 (1994).
24. Altschuler, Y. *et al.* ADP-ribosylation factor 6 and endocytosis at the apical surface of Madin-Darby canine kidney cells. *J. Cell Biol.* **147,** 7–12 (1999).
25. Shurety, W., Bright, N. A. & Luzio, J. P. The effects of cytochalasin D and phorbol myristate acetate on the apical endocytosis of ricin in polarised Caco-2 cells. *J. Cell Sci.* **109,** 2927–2935 (1996).
26. Hyman, T., Shmuel, M. & Altschuler, Y. Actin is required for endocytosis at the apical surface of Madin-Darby canine kidney cells where ARF6 and clathrin regulate the actin cytoskeleton. *Mol. Biol. Cell* **17,** 427–437 (2006).
27. Da Costa, S. R. *et al.* Impairing actin filament or syndapin functions promotes accumulation of clathrin-coated vesicles at the apical plasma membrane of acinar epithelial cells. *Mol. Biol. Cell* **14,** 4397–4413 (2003).
28. Shmuel, M. *et al.* ARNO through its coiled-coil domain regulates endocytosis at the apical surface of polarized epithelial cells. *J. Biol. Chem.* **281,** 13300–13308 (2006).
29. Buss, F., Arden, S. D., Lindsay, M., Luzio, J. P. & Kendrick-Jones, J. Myosin VI isoform localized to clathrin-coated vesicles with a role in clathrin-mediated endocytosis. *EMBO J.* **20,** 3676–3684 (2001).
30. Poupon, V. *et al.* Clathrin light chains function in mannose phosphate receptor trafficking via regulation of actin assembly. *Proc. Natl Acad. Sci. USA* **105,** 168–173 (2008).
31. Macia, E. *et al.* Dynasore, a cell-permeable inhibitor of dynamin. *Dev. Cell* **10,** 839–850 (2006).

32. Rohatgi, R. *et al*. The interaction between N-WASP and the Arp2/3 complex links Cdc42-dependent signals to actin assembly. *Cell* **97,** 221–231 (1999).
33. Paleotti, O. *et al*. The small G-protein ARF6GTP recruits the AP-2 adaptor complex to membranes. *J. Biol. Chem.* **280,** 21661–21666 (2005).
34. Chen, C.-Y. & Brodsky, F. M. Huntingtin-interacting protein 1 (Hip1) and Hip1-related protein (Hip1R) bind the conserved sequence of clathrin light chains and thereby influence clathrin assembly *in vitro* and actin distribution *in vivo*. *J. Biol. Chem.* **280,** 6109–6117 (2005).
35. Engqvist-Goldstein, A. E. *et al*. The actin-binding protein Hip1R associates with clathrin during early stages of endocytosis and promotes clathrin assembly *in vitro*. *J. Cell Biol.* **154,** 1209–1223 (2001).
36. Wilbur, J. D. *et al*. Actin binding by Hip1 (huntingtin-interacting protein 1) and Hip1R (Hip1-related protein) is regulated by clathrin light chain. *J. Biol. Chem.* **283,** 32870–32879 (2008).
37. Engqvist-Goldstein, A. E. *et al*. RNAi-mediated Hip1R silencing results in stable association between the endocytic machinery and the actin assembly machinery. *Mol. Biol. Cell* **15,** 1666–1679 (2004).
38. Dai, J. & Sheetz, M. P. Membrane tether formation from blebbing cells. *Biophys. J.* **77,** 3363–3370 (1999).
39. Fotin, A. *et al*. Structure determination of clathrin coats to subnanometer resolution by single particle cryo-electron microscopy. *J. Struct. Biol.* **156,** 453–460 (2006).

DOI: 10.1038/ncb2307

METHODS

Reagents. Rabbit polyclonal antibodies against dynamin-2 (Hudy-1, Millipore; 1:1,000), villin (provided by M. Arpin; 1:2,000) and ezrin (Cell Signaling Technology; 1:1,000), mouse monoclonal antibodies against ZO-1 (Invitrogen; 1:2,000) and clathrin light chains (CON-1 generated from hybridoma cells; 1:500), and Alexa Fluor 488, 546 or 647 secondary antibodies and Alexa 647 human-transferrin (Molecular Probes/Invitrogen; 1:1,000) were used.

Jasplakinolide (Alexis Biochemical), latrunculin A, NSC-23766 (Rac1 inhibitor[40]), SecinH3 (inhibitor for cytohesins[41], small guanine nucleotide exchange factors (GEFs) for Arf factors including Arf6; Calbiochem) and secramine (inhibitor of Cdc42; ref. 42) were used at 1 μM, 1 μM, 50 μM and 1 μM, respectively.

Cell culture and transfections. MDCK and BSC1 cells stably expressing σ2–eGFP (the small subunit of AP-2 fused to enhanced green fluorescent protein, eGFP) were grown in DMEM medium containing 10% FCS, penicillin and streptomycin. The MDCK cells expressing σ2–eGFP were generated by transfection with Fugen HD selected with G418. Plasmids encoding Cherry fused to wild-type and mutant bovine clathrin light chain B (Cherry–LCb and Cherry–LCb-EED/QQN) were made by exchange of eGFP with Cherry from eGFP–LCb and eGFP–LCb-EED/QQN (P. McPherson). Transient expression of villin–Cherry, Cherry–LCb and Cherry–LCb-EED/QQN was carried out using TransIT-LT1 (Mirus Bio LL) and cells were analysed 12–16 h after transfection unless otherwise indicated.

Gene silencing. Simultaneous depletion of clathrin light chains A and B was achieved in MDCK cells stably expressing σ2–eGFP by siRNA-mediated gene silencing as described previously[11].

Depletion of villin-1 and ezrin was achieved by shRNA. siRNA sequences specific for villin-1 (5′-CCGGGCCAAGATGAAATTACAGCATCTCG-AGATGCTGTAATTTCATCTTGGCTTTTTG-3′) and ezrin genes 5′-CCGGCCTG-GAAATGTATGGAATCAACTCGAGTTGATTCCATACATTTCCAGGTTTTTG-3′) were incorporated into the lentivirus vector pLKO.1 (Addgene). MDCK cells (1×10^6) stably expressing σ2–eGFP were transduced with 50–100 μl of thawed supernatants, and cells containing integrated viral sequences were selected by serial passage in medium containing 4 μg ml^{-1} puromycin.

Osmotic swelling. MDCK or BSC1 cells kept at 37 °C and in the presence of humidified 5% CO_2 were exposed for 10 min to diluted medium (311, 251, 220 and 174 mOsM) prepared by mixing 100, 80, 70 or 50% of phenol red-free DMEM containing 10% FCS serum with 0, 20, 30 or 50% water containing 10% FCS serum. Live-cell imaging time series were acquired immediately before and after the hypo-osmotic treatment. In some experiments, jasplakinolide was added after 10 min of exposure to the hypotonic medium; in other experiments, jasplakinolide was included before and during the treatment with the hypotonic medium. Both protocols elicited the same actin dependence on the dynamics of clathrin coat formation. The actin dependence imparted by osmotic swelling of cells incubated for 10 min with 50% medium was fully lost on incubation for 10 min with normal medium.

Controlled stretching. To form the support chamber, first a thin sheet of polydimethylsiloxane (PDMS; 50 μm in thickness; Specialty Silicone Products) was placed on the bottom of a 35-mm-diameter glass Petri dish. An optically flat-ended fused silica rod (Techspec, Edmund Optics) was placed on top of the PDMS sheet and used to cast the lateral walls of the PDMS chamber. The chamber was made by pouring PDMS (Sylgard 184 silicone elastomer kit; Ellsworth Adhesives) degassed for about 20 min until no more bubbles formed, and then cured for 2 h at 65 °C. After extensive washes with water, the PDMS sheet was coated overnight at 4 °C with 50 μg ml^{-1} fibronectin (dissolved in water) and then washed once more with PBS. About 1×10^4 cells were plated for 16 h at 37 °C. The PDMS chamber with cells was attached to a 37 °C pre-equilibrated stretching device equipped with a micrometre screw and then mounted on the temperature-controlled stage of the microscope. Imaging was done before and immediately after ∼25% mechanical stretching along one horizontal axis.

Immunofluorescence microscopy. Cells were fixed for 15 min at room temperature with 4% w/v paraformaldehyde in PBS, followed by sequential incubation with primary and secondary antibodies in PBS containing 0.05% w/v Triton X-100 and 2% FCS.

Electron microscopy. Electron microscopy was carried out as described previously[10].

Live-cell spinning-disc confocal imaging. About 1×10^5 BSC1 cells were plated 16 h before imaging on 25-mm-diameter glass No. 1.5 coverslips; a similar number of MDCK cells were plated 1 day or 3 days (to allow for cell polarization) before imaging. Imaging medium was phenol red-free DMEM with 10% FCS and 20 mM HEPES. For imaging, the coverslips were placed on a temperature-controlled 5% CO_2-humidified chamber (20/20 Technologies) mounted on the stage of a Mariana imaging system (Intelligent Imaging Innovations) based on an Axiovert 200 M inverted microscope (Carl Zeiss), a CSU-X1 spinning-disc confocal unit (Yokogawa Electric Corporation), a spherical-aberration-correction device (SAC; Infinity Photo-Optical) and a ×63 objective lens (Plan-Apochromat, NA 1.4, Carl Zeiss)[10]. The SAC resolved the severe spherical aberration especially noticeable on the apical surface located 8–10 μm away from the coverslip using SAC values of 1,100 and 850 for basolateral/bottom and apical surfaces of cells on glass coverslips, and 0 for bottom (attached) surfaces of cells on PDMS. Two-dimensional (2D) and 3D time series were obtained using Slidebook 5 (3I).

Data acquisition, image processing and statistical analysis. 2D movies from the attached surfaces (basolateral for polarized and ventral for non-polarized cells) were obtained with 100 ms exposures from a single optical plane. 3D movies from the free surface (apical for polarized and dorsal for non-polarized) correspond to z stacks of 3–5 consecutive optical planes spaced 0.5 μm acquired at a frequency of 0.5 Hz per stack and 100 ms exposure; a 2D movie was then obtained by generating for each time point a maximum-intensity z projection. The 3D movies had a duration of 120–160 s, sufficient to fully track the few non-arrested AP-2 spots; the remaining ones had lifetimes longer than 10 min when stalled by the absence of actin dynamics. Time series from the bottom surface were acquired from a single optical plane because the intensity and lifetime data obtained from these 2D movies were equivalent to data obtained from 3D movies, thus minimizing potential photobleaching and phototoxicity effects.

AP-2 spots were identified and tracked using a MATLAB routine (Kural, C., Boulant, S. & Kirchhausen, T., manuscript in preparation) using three sequential steps composed of 2D Gaussian and Laplacian filtering followed by a local maxima-finding algorithm. The intensity profile as a function of time was used to characterize the dynamics of each of the AP-2 spots selected according to the following criteria: fluorescent objects were diffraction limited; dynamic, non-arrested objects appeared and disappeared within the time window of the time series with lifetimes of at least 20 s (thus, shorter-lived objects corresponding to abortive pits were not included for analysis); arrested objects were those present throughout the duration of the time series; the fluorescent objects did not collide with each other.

Statistical tests. The statistical significance for the differences between the lifetime or maximum fluorescence intensity of the data determined under specific experimental conditions was established using a two-tailed Student t-test.

Estimate of the work required to deform a membrane vesicle under conditions of membrane tension. We estimate the work done against tension as the product of the tension and the net increase in membrane area required to advance the bud to the point in question. During budding of the initial hemisphere, the increase in membrane area in the pit is accompanied by a decrease in area in the plane of the cell surface. However, when the membrane starts to constrict, both areas increase together (Fig. 5). Measured membrane tensions for cells in culture are in the range 10–50 mN m^{-1}. To generate a typical coated pit, which encloses a vesicle of diameter ∼700 Å in a shell of about 60–80 clathrin trimers (∼200 heavy chains), from a membrane under 30 mN m^{-1} tension, the work needed to form the first hemisphere is about 10^{-19} J or 60 kJ mol^{-1} (15 kcal mol^{-1}), whereas the work needed to complete the second hemisphere is three times that value. If 100 heavy chains contribute to the lattice surrounding the initial hemisphere, the corresponding membrane deformation requires only about 0.6 kJ mol^{-1} of net free energy per heavy chain beyond the free energy needed to generate a membrane-free clathrin lattice—that is, a contribution considerably less than $k_B T$, where k_B is Boltzmann's constant and T is temperature. Note that the estimated work required to bend a membrane into a hemisphere is roughly ten times this amount, but still only the equivalent of 1–2 well-placed hydrogen bonds per heavy chain and therefore easily within the free energy likely to come from assembly of the clathrin lattice. If the tension rises 10-fold (from cytoskeletal stretching, osmotic changes and so on), to levels comparable to the tension of cytoskeletally constrained red blood cell membranes[38,43], the work needed to overcome tension becomes comparable to the bending work. Our observations indicate that in the absence of actin dynamics this contribution is enough to stall invagination. Addition of one actin monomer to a growing filament generates a force of about 10 pN (refs 44,45) and a displacement at the tip by about 3 nm, for example about 3×10^{-20} J or 18 kJ mol^{-1}. Thus, the addition of about 20 actin monomers

to each of 5–10 filaments can do more than enough work, in concert with the contribution from clathrin polymerization, to deform the second hemisphere and to displace the invaginating membrane by about 60 nm—nearly a full vesicle diameter.

40. Gao, Y., Dickerson, J. B., Guo, F., Zheng, J. & Zheng, Y. Rational design and characterization of a Rac GTPase-specific small molecule inhibitor. *Proc. Natl Acad. Sci. USA* **101,** 7618–7623 (2004).
41. Hafner, M. *et al.* Inhibition of cytohesins by SecinH3 leads to hepatic insulin resistance. *Nature* **444,** 941–944 (2006).
42. Pelish, H. E. *et al.* Secramine inhibits Cdc42-dependent functions in cells and Cdc42 activation *in vitro*. *Nat. Chem. Biol.* **2,** 39–46 (2006).
43. Hochmuth, F. M., Shao, J. Y., Dai, J. & Sheetz, M. P. Deformation and flow of membrane into tethers extracted from neuronal growth cones. *Biophys. J.* **70,** 358–369 (1996).
44. Noireaux, V. *et al.* Growing an actin gel on spherical surfaces. *Biophys. J.* **78,** 1643–1654 (2000).
45. Upadhyaya, A., Chabot, J. R., Andreeva, A., Samadani, A. & van Oudenaarden, A. Probing polymerization forces by using actin-propelled lipid vesicles. *Proc. Natl Acad. Sci. USA* **100,** 4521–4526 (2003).